A 3-Dimensional Numerical Thermal Analysis for A Vertical Double U-Tube Ground-Coupled Heat Pump

Ali H. Tarrad

***Abstract*—The ground heat exchanger plays a major role in the thermal performance and economic optimization of the ground-coupled heat pump. The present study focuses on the effect of the borehole size and the grout and soil thermal properties on the thermal assessment of these heat exchangers. A double U-tube heat exchanger was studied numerically by the COMSOL Multiphysics 5.4 software in a 3-dimensional discretization model. The double U-tube was circuited as a parallel flow arrangement and situated in a parallel configuration (PFPD) deep in the borehole. The grout and ground thermal conductivities were selected in the range of (0.73-2.0) W/m.K and (1.24-2.8) W/m.K respectively. The results revealed that the ground thermal conductivity showed a more pronounced influence on the thermal performance of the ground heat exchanger and with less extent for the grouting one. Increasing the grout filling thermal conductivity from (0.73) W/m.K to (2.0) W/m.K at a fixed ground thermal conductivity of (2.4) W/m.K has augmented the heat transfer rate by (10) %. The heat transfer rate of the ground heat exchanger exhibited marked enhancement as much as double when the ground thermal conductivity was increased from (1.24) W/m.K to (2.8) W/m.K at fixed grout thermal conductivity range of (0.78-2.0) W/m.K. It has been verified that increasing the borehole size has a negligible effect on the ground heat exchanger thermal performance when a grout with a high thermal conductivity was utilized in the ranged of examined configurations. The steady-state numerical analysis model outcomes of the present work could be implemented for the preliminary borehole design for a ground heat exchanger.**

***Index Terms*—3-Dimensional analysis, thermal assessment, vertical double U-tube, borehole size, a steady-state condition.**

I. INTRODUCTION

The understanding of such topics of heat transfer took a deep consideration in the experimental, analytical, and numerical research by scientists, Ingersoll *et al*. [1], Carslaw and Jaeger [2], Kavanaugh [3], Zeng *et al*. [4], and Muttil and Chau [5]. The equivalent single tube replacement for the U-tube and concentric positioning in the borehole for the prediction of the borehole thermal resistance has been implemented by several researchers, Claesson and Dunand [6], Shonder and Beck [7], Gu and O'Neal [8], and Tarrad [9]-[12]. A 2-dimensional time-dependent numerical model was accomplished to consider the heat flow in the ground by Zeng and Fang [13] and Zeng *et al*. [14]. This was because the temperature variation inside the borehole is usually slow and minor. Li and Zheng [15] considered different soil layers and developed a 3-dimensional finite-volume model for a vertical ground heat exchanger. Zanchini *et al*. [16], [17] utilized the COMSOL Multiphysics 3.4 software to study the effects of flow direction and thermal short-circuiting on the performance of small and 100 m long coaxial ground heat exchangers. More recently, Tarrad [18] studied the effect of the number of U-tubes inside the borehole on thermal performance. A 3-dimensional model was built by the implementation of the COMSOL Multiphysics 5.4 software. He concluded that the heat transfer rate of the double U-tube was better than that of the single one by (10-14) % when operates at the same total fluid mass flow rate and inlet temperature for a given borehole design.

In the present work, a steady-state 3-dimensional mode for the ground U-tube heat exchanger accomplished by the COMSOL Multiphysics 5.4 software [19] is presented.

Manuscript received May 18, 20212021; revised May 27, 2021.

A. H. Tarrad is with the Université de Lorraine, CNRS, LEMTA, Nancy, France (e-mail: ali.tarrad@univ-lorraine.fr).

II. PRESENT MODEL

A. Borehole Characteristics

The tube geometry, grout filling, and soil characteristics are listed in Table I.

TABLE I: PHYSICAL DIMENSIONS OF DIFFERENT ZONES

Zone Material	Parameter	Value
(HDPE)* High density polyethylene pipe	(d_o), (mm)	33.4
	(d_i), (mm)	29.5
	(tp), (mm)	2.0
	(WF), (---)	17
	(S_p), (mm)	66.8
	($H_{U\text{-}tube}$), (m)	35.1
Borehole (Grout)	(D_b), (mm)	120-160
	(H_b), (m)	35.2
Soil	(D_s), (m)	5.0
	(H_s) (m)	37.7

* Dimensional data for the tube were taken from reference [18].

B. Materials and Thermal Properties

The U-tube was made of high-density polyethylene with thermal conductivity, density, and specific heat of (0.4) W/m.K, (940) kg/m^{3,} and (2.3) kJ/kg respectively. The thermal properties of selected materials utilized in the present work are illustrated in Table II.

TABLE II.A: THERMAL CONDUCTIVITY OF GROUT MIXTURES

Grouts	k (W/m K)	ρ (kg/m^3)	cp (kJ/kg K)
20% Bentonite [20]	0.728	1096	3.743
Cement Mortar [21]	0.78	1000	1.6
20% Bentonite/20 % Silica Sand [20]	0.855	1298	2.960
20% Bentonite/30 % Silica Sand [20]	0.988	1354	2.770
30% Bentonite/30 % Silica	1.127	1439	2.519

doi: 10.18178/ijcea.2021.12.2.789

Sand [20]			
30% Bentonite – 30% Quartzite [22]	1.3	-----	-----
30% Bentonite – 40% Quartzite [3]	1.47	-----	-----
Bentonite Grout [23]	1.6	2600	0.720
60% Quartzite- Flowable Fill [22] (Cement + Fly Ash + Sand)	1.85	-----	-----
Sand [23]	2.0	2500	1.110

TABLE II.B: THERMAL PROPERTIES OF GROUND

Ground	k (W/m K)	ρ (kg/m^3)	cp (kJ/kg K)	$\rho\ cp$ (MJ/m^3 K)
Ref. [24]	1.24	1588	1.465	2.3264
Ref. [25]	1.4	2200	0.91	2.002
Ref. [23]	2.0	2183	0.996	2.1743
Ref. [21, 18]	2.42	2800	0.84	2.352
Ref. [25]	2.8	2200	0.91	2.002

C. Configuration and Mesh Generation

A schematic presentation for the double U-tube installation in the borehole is shown in Fig. 1 for the (PFPD) arrangement.

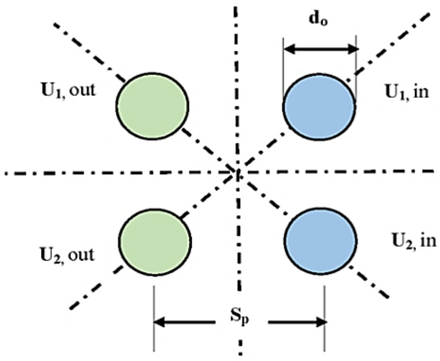

Fig. 1. A schematic diagram for the model double U-tube.

The temperature at the far distance boundary and the bottom part of the borehole soil was fixed at (16) ℃ from the ground surface down to the bottom of the soil domain at (37.6) m. The ground surface was assigned as an adiabatic boundary. Water was chosen as a carrier fluid, it enters the U-tube at a temperature of (33) ℃ and a mass flow rate of (0.68) kg/s. The total mass flow rate was divided equally between the two U-tubes to constitute a parallel flow circuiting each with (0.34) kg/s and produces a flow velocity of (0.5) m/s. The low Reynolds ($\kappa - \varepsilon$) turbulence module was implemented as described in [19]. A free tetrahedral element type was used for mesh generation, the fluid and grout domains were discretized in finer element sizes than that of the soil domain, Fig. 2.

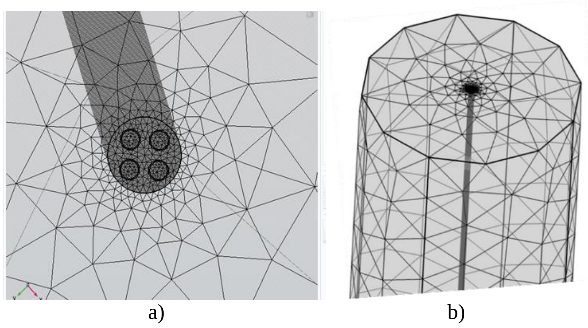

a) b)

Fig. 2. a) The generated mesh of the borehole geometry; b) A general view for the model mesh generation.

D. Mathematical Representation

The mathematical and physical phenomena of the present model are stated in appendix (A). It illustrates the general forms of the expressions that control the fluid dynamics and heat transfer for the carrier fluid as represented by the continuity, Navier-Stokes, and energy relations. The energy equation for all of the solid domains is expressed in terms of Fourier's law.

III. DATA REDUCTION

The water temperature monitoring with depth was conducted during the numerical thermal assessment of the borehole. The dissipated heat load to the ground by the water cooling process was estimated from:

$$\dot{Q}_{H.E} = \dot{m_w}\, c_{p,w}\, \Delta T_w \tag{1}$$

The water temperature drop between the entering and discharge ports of the heat exchanger was represented as:

$$\Delta T_w = T_{w,in} - T_{w,out} \tag{2}$$

The heat loading of the heat exchanger corresponds to the capability of the borehole to dissipate heat to the ground in terms of the borehole depth, it was predicted from:

$$q_{l,H.E} = \frac{\dot{Q}_{H.E}}{L} \tag{3}$$

The total borehole thermal resistance was obtained from the general form of Fourier's law as:

$$R_{t,m} = \frac{T_{w,m} - T_S}{q_l} \tag{4}$$

In this expression, the mean water temperature ($T_{w,m}$) was estimated from:

$$T_{w,m} = \frac{T_{w,in} + T_{w,out}}{2} \tag{5}$$

Finally, the deviation percentage of any thermal performance parameter was estimated by:

$$\xi_{H.E} = \frac{\psi_{H.E} - \psi_{ref}}{\psi_{H.E}} \times 100 \tag{6}$$

In this expression, the parameter (ψ) represents any thermal performance variable as ($\dot{Q}_{H.E}$), (ΔT_w), ($q_{l,H.E}$) and ($R_{t,m}$).

IV. RESULTS AND DISCUSSION

A. Grout/Ground Thermal Effect

Fig. 3 depicts the heat transfer performance of the double U-tube heat exchangers as a function of grout thermal conductivity at fixed soil thermal conductivity of (2.42) W/m.K.

The rejected heat transfer rate to the ground region showed an augmentation with grout thermal conductivity. Increasing the grout thermal conductivity from (0.73) W/m.K to (2.0) W/m.K has enhanced the heat transfer rate and reduced the total borehole thermal resistance by (10) %.

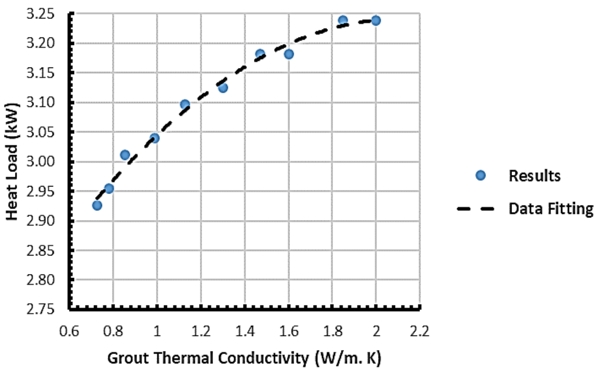

a)

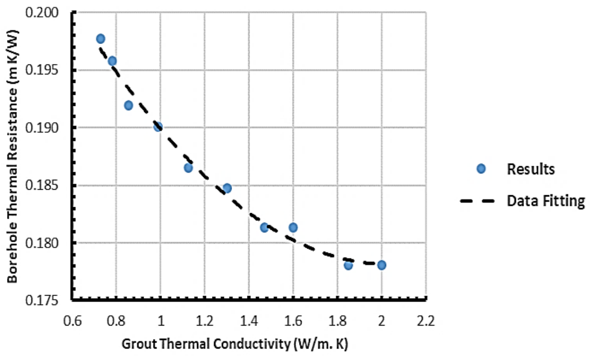

b)

Fig. 3. a) Heat load variation with grout thermal conductivity at soil thermal conductivity of (2.42) W/m.K; b) Borehole thermal resistance variation with grout thermal conductivity at soil thermal conductivity of (2.42) W/m.K.

The soil thermal conductivity exhibited a marked influence on the thermal performance of the ground U-tube heat exchanger, Fig. 4.

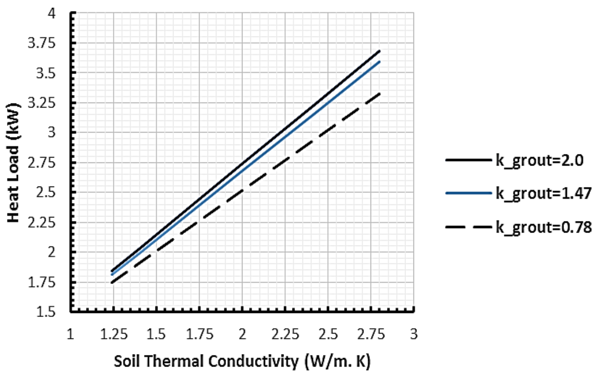

a)

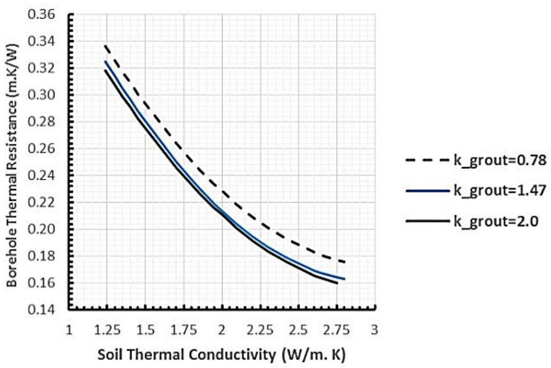

b)

Fig. 4. a) Heat load variation with soil thermal conductivity; b) Total borehole thermal resistance variation with soil thermal conductivity.

Increasing the soil thermal conductivity from (1.24) W/m.K to (2.8) W/m.K has doubled the borehole heat transfer rate and almost halved the total borehole thermal resistance. The heat load of the borehole showed a linear augmentation with the soil thermal conductivity and the higher load was achieved at the examined (2.8) W/m.K thermal conductivity value. Higher heat transfer rates were experienced at grout thermal conductivity of (1.47) W/m.K and (2.0) W/m.K than that of the (0.78) W/m.K for all of the examined range of soil thermal conductivity.

The heat loading of the U-tube heat exchanger at a fixed ground thermal conductivity of (2.42) W/m.K reached values in the range of (83-92) W/m for grout thermal conductivity range (0.73-2.0) W/m.K, Fig. 5.a. The soil thermal conductivity range of (1.24-2.8) W/m.K and grout thermal conductivity of (2.0) W/m.K achieved a heat loading of (52-104) W/m, Fig. 5.b.

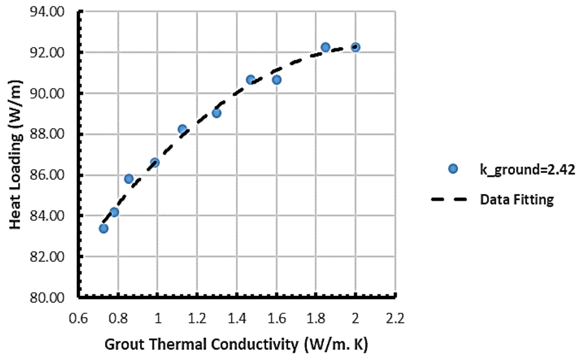

a)

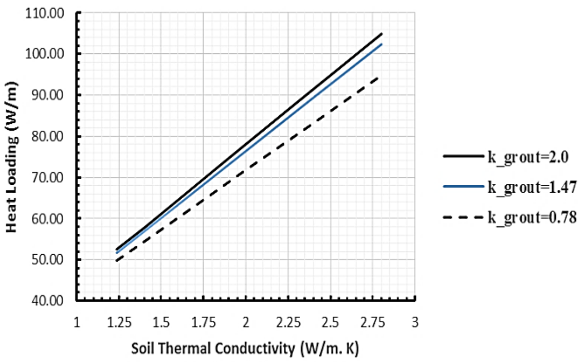

b)

Fig. 5. a) Heat loading variation with grout thermal conductivity; b) Heat loading variation with soil thermal conductivity.

B. Borehole Size

The borehole diameter showed a negligible effect at higher grout thermal conductivity than that of the low values. Increasing the configuration factor *(β)* from (0.42) to (0.56) corresponds to decreasing the borehole diameter from (160) mm to (120) mm at (S_p) of (66.8) mm as defined by:

$$\beta = \frac{S_p}{D_b} \tag{7}$$

Fig. 6 depicts the predicted heat load at a variety of configuration factors of the U-tube heat exchanger. As the configuration factor (β) increases, the tube boundary will be situated close to the borehole wall and hence improves the heat transfer rate of the heat exchanger.

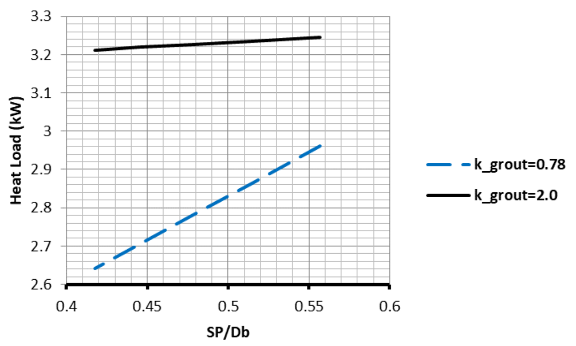

Fig. 6. Borehole heat load variation with configuration factor at soil thermal conductivity of (2.42) W/m.K.

For a grout thermal conductivity of (0.78) W/m.K, a value of (11) % of heat transfer enhancement was achieved when the configuration factor increased from (0.42) to (0.56). For the case of (2.0) W/m.K grout thermal conductivity, the effect of (β) was negligible and the enhancement was only (1) %. This is due to the thin layer of grout that surrounds the tube surface and hence the thermal conductivity of the filling has a minor effect on the heat transfer process. However, the higher grout thermal conductivity produced a higher heat transfer rate than that of the low one by a range fell within (9-18) %, Fig. 6. The heat loading at (2.0) W/m.K grout thermal conductivity was about (92) W/m but it fell within the range (75-84) W/m for the low thermal conductivity one in the examined range of (β).

V. Conclusion

A thermal assessment by a numerical 3-dimensional model was accomplished for a double U-tube circuited in a parallel flow/parallel installation (PFPD) in the borehole. Increasing the thermal conductivity of the grout filling improved the rate of the dissipated load to the ground domain. The heat load and hence the heat loading of the U-tube was enhanced by (10) % when the thermal conductivity of the grout was increased from (0.73) W/m.K to (2.0) W/m.K at a fixed ground thermal conductivity of (2.42) W/m.K. For a constant grout thermal conductivity, the soil showed a marked increase for the heat load. Increasing the soil thermal conductivity from (1.24) W/m.K to (2.8) W/m.K has doubled the borehole heat transfer rate and almost halved the total borehole thermal resistance. For the examined configuration conditions, it has been verified that increasing the borehole size has a negligible effect on the ground heat exchanger thermal performance when a grout with a high thermal conductivity was utilized.

Nomenclature

Parameter	Definition
cp	Specific heat, (kJ/kg)
d	Tube diameter, (mm)
D	Diameter, (mm)
g	Gravitational acceleration, (m/s^2)
H	Borehole depth, (m)
k	Thermal conductivity, (W/m.K)
L	Length, (m)
$\dot{m}$	Mass flow rate, (kg/s)
p	Pressure, (Pa) or (bar)
$\acute{q}$	Heat generation per unit volume, (W/m^3)
q_l	Heat loading, (W/m)
$\dot{Q}$	Heat transfer rate, (kW)
r, θ, z	Cylindrical-coordinate variables
R	Thermal resistance per meter, (m.K/W)
S_p	U-tube legs spacing, (mm)
T	Temperature (K)
ΔT	Temperature difference, (K)
u_r, u_θ, u_z	Cylindrical velocity components, (m/s)
v	Water flow velocity, (m/s)

Subscripts

Subscript	Definition
b	Borehole
g	Grout
$H.E$	Heat exchanger
i	Inside
in	Inlet
m	mean
o	Outside
out	Outlet
p	Pipe
ref	Reference Arrangement
s	Soil or ground
t	Total
w	Water

Greek Letters

Parameter	Definition
α	Thermal diffusivity, (m^2/s)
β	Configuration factor, (---)
ε	Dissipation rate of turbulent kinetic energy, m^2/s^3
κ	Turbulent kinetic energy, m^2/s^2
ξ	Deviation percentage, %
μ	Fluid dynamic viscosity, Pa.s
$\boldsymbol{\rho}$	Density, (kg/m^3)
Φ	Viscous dissipation rate, N/(m^2 s)
ψ	Performance parameter in eq. (6)

Appendix (A)

Fluid Domain

The fluid domain is described by the mathematical expressions of the conservation equations, continuity, Navier-Stokes, and energy in an incompressible flow as cited in Bird *et al.* [26]:

A. Continuity Equation

$$\frac{1}{r}\frac{\partial\,(r\,u_r)}{\partial r}+\frac{1}{r}\frac{\partial u_\theta}{\partial \theta}+\frac{\partial u_z}{\partial z}=0 \qquad \text{(A.1)}$$

B. Navier-Stokes Equation

$$\rho\left(\frac{\partial u_r}{\partial t}+u_r\frac{\partial u_r}{\partial r}+\frac{u_\theta}{r}\frac{\partial u_r}{\partial \theta}+u_z\frac{\partial u_r}{\partial z}-\frac{{u_\theta}^2}{r}\right)=\rho g_r-\frac{\partial p}{\partial r}+\mu\left[\frac{1}{r}\frac{\partial}{\partial r}\left(r\frac{\partial u_r}{\partial r}\right)+\frac{1}{r^2}\frac{\partial^2 u_r}{\partial \theta^2}+\frac{\partial^2 u_r}{\partial z^2}-\frac{2}{r^2}\frac{\partial u_\theta}{\partial \theta}-\frac{u_r}{r^2}\right] \qquad \text{(A.2.a)}$$

$$\rho\left(\frac{\partial u_\theta}{\partial t}+u_r\frac{\partial u_\theta}{\partial r}+\frac{u_\theta}{r}\frac{\partial u_\theta}{\partial \theta}+u_z\frac{\partial u_\theta}{\partial z}+\frac{u_r\,u_\theta}{r}\right)=\rho g_\theta-\frac{1}{r}\frac{\partial p}{\partial \theta}+\mu\left[\begin{array}{c}\frac{1}{r}\frac{\partial}{\partial r}\left(r\frac{\partial u_\theta}{\partial r}\right)+\frac{1}{r^2}\frac{\partial^2 u_\theta}{\partial \theta^2}+\frac{\partial^2 u_\theta}{\partial z^2}+\\ \frac{2}{r^2}\frac{\partial u_r}{\partial \theta}-\frac{u_\theta}{r^2}\end{array}\right] \qquad \text{(A.2.b)}$$

$$\rho\left(\frac{\partial u_z}{\partial t}+u_r\frac{\partial u_z}{\partial r}+\frac{u_\theta}{r}\frac{\partial u_z}{\partial \theta}+u_z\frac{\partial u_z}{\partial z}\right)=\rho g_z-\frac{\partial p}{\partial \theta}+\mu\left[\frac{1}{r}\frac{\partial}{\partial r}\left(r\frac{\partial u_z}{\partial r}\right)+\frac{1}{r^2}\frac{\partial^2 u_z}{\partial \theta^2}+\frac{\partial^2 u_z}{\partial z^2}\right] \qquad \text{(A.2.c)}$$

C. Energy Equation

$$\frac{\partial T}{\partial t}+u_r\frac{\partial T}{\partial r}+\frac{u_\theta}{r}\frac{\partial T}{\partial \theta}+u_z\frac{\partial T}{\partial z}=\frac{\acute{q}}{cp}+\alpha\left[\frac{1}{r}\frac{\partial}{\partial r}\left(r\frac{\partial T}{\partial r}\right)+\frac{1}{r^2}\frac{\partial^2 T}{\partial \theta^2}+\frac{\partial^2 T}{\partial z^2}\right]+\frac{\Phi}{\rho\,cp} \qquad \text{(A.3.a)}$$

where the viscous dissipation rate is:

$$\Phi = 2\,\mu\left[\left(\frac{\partial u_r}{\partial r}\right)^2 + \left(\frac{1}{r}\,\frac{\partial u_\theta}{\partial \theta} + \frac{u_r}{r}\right)^2 + \left(\frac{\partial u_z}{\partial z}\right)^2\right] + \mu\left[\left(\frac{1}{r}\,\frac{\partial u_r}{\partial \theta} + \frac{\partial u_\theta}{\partial r} - \frac{u_\theta}{r}\right)^2 + \left(\frac{\partial u_\theta}{\partial z} + \frac{1}{r}\,\frac{\partial u_z}{\partial \theta}\right)^2 + \left(\frac{\partial u_z}{\partial r} + \frac{\partial u_r}{\partial z}\right)^2\right] \tag{A.3.b}$$

These equations represent the complete forms of the handled expressions in the fluid domain for the transient mode. In the present model, the time-dependent parameters were dropped together with the heat generation ($\acute{q}$) and gravity terms (ρg).

Solid Domains

The general Fourier's law is applicable in the solid domains of the model, tube wall, grout, and soil:

$$\frac{1}{r}\,\frac{\partial}{\partial r}\left(r\,\frac{\partial T}{\partial r}\right) + \frac{1}{r^2}\,\frac{\partial}{\partial \theta}\left(r\,\frac{\partial T}{\partial \theta}\right) + \frac{\partial}{\partial z}\left(\frac{\partial T}{\partial z}\right) + \acute{q} = \frac{1}{\alpha}\,\frac{\partial T}{\partial t} \tag{A.4}$$

The energy generation per unit volume ($\acute{q}$) and the temperature variation with time set to zero for a steady-state condition.

Acknowledgment

The author expresses his sincere thanks to the administration of (PAUSE) program in France and the University of Lorraine for their valuable and endless support to complete this work. Thanks are due to Professor Pascal Boulet, the director of the Laboratoire Énergies & Mécanique Théorique et Appliquée (LEMTA) for his unlimited support and encouragement.

Conflict of Interest

The author declares that there is no conflict of interest.

References

[1] L. R. Ingersoll, O. J. Zobel, and A. C. Ingersoll, *Heat Conduction with Engineering, Geological and Other Applications*, revised edition; University of Wisconsin Press: Madison, 1954.

[2] H. S. Carslaw and J. C. Jaeger, *Conduction of Heat in Solids*, 2nd ed. Oxford University Press: London, 1959.

[3] S. Kavanaugh, "Simulation and experimental verification of vertical ground coupled heat pump systems," PhD. thesis, Oklahoma State University, USA, 1985.

[4] H. Zeng, N. Diao, and Z. Fang, "Heat transfer analysis of boreholes in vertical ground heat exchangers," *International Journal of Heat and Mass Transfer*, vol. 46, pp. 4467-4481, 2003.

[5] N. Muttil and K. W. Chau, "Neural network and genetic programming for modeling coastal algal blooms," *Int. J. Environ. Pollution*, vol. 28, pp. 223-238, 2006.

[6] J. Claesson and A. Dunand, "Heat extraction from the ground by horizontal pipes—A mathematical analysis," Document D1, Swedish Council for Building Research, Stockholm, 1983.

[7] J. A. Shonder and J. V. Beck, "Determining effective soil formation thermal properties from field data using a parameter estimation technique," *ASHRAE Transactions*, vol. 105, pp. 458-466, 1999.

[8] Y. Gu and D. L. O'Neal, "Development of an equivalent diameter expression for vertical U-tubes used in ground-coupled heat pumps," *ASHRAE Transaction*, vol. 104, no. 2- 4214, pp. 1-9, 1998.

[9] A. H. Tarrad, "A borehole thermal resistance correlation for a single vertical DX U-tube in geothermal energy application," *American Journal of Environmental Science and Engineering*, vol. 3, no. 4, pp. 75-83, 2019.

[10] A. H. Tarrad, "A perspective model for borehole thermal resistance prediction of a vertical U-tube in geothermal heat source," *Athens Journal of Technology and Engineering*, vol. 7, no. 2, pp. 73-92, 2020.

[11] A. H. Tarrad, "Development of analytical model for a vertical single U-tube ground-coupled heat pump system," *Global Journal of Researches in Engineering: General Engineering*, vol. 20, no. 3, version 1.0, pp. 1-14, 2020.

[12] A. H. Tarrad, "A simplified thermal design model for a single vertical U-tube borehole utilized in ground-coupled source heat pumps," *International Journal of Scientific Research in Computer Science, Engineering and Information Technology (IJSRCSEIT)*, vol. 6, no. 5, pp. 151-162, 2020.

[13] H. Zeng and Z. Fang, "A fluid temperature model for vertical U-tube geothermal heat exchangers," *Journal of Shandong Institute of Architecture and Engineering*, vol. 17, no. 1, pp. 7-10, 2002.

[14] H. Zeng, N. Diao, and Z. Fang, "A finite line-source model for boreholes in geothermal heat exchangers," *Heat Transfer – Asian Research*, vol. 31, no. 7, pp. 558-567, 2002.

[15] Z. Li and M. Zheng, "Development of a numerical model for the simulation of vertical U-tube ground heat exchangers," *Applied Thermal Engineering*, vol. 29, no. 5, pp. 920-924, 2009.

[16] E. Zanchini, S. Lazzari, and A. Priarone, "Effects of flow direction and thermal short-circuiting on the performance of small coaxial ground heat exchangers," *Renewable Energy*, vol. 35, pp. 1255–1265, 2010.

[17] E. Zanchini, S. Lazzari, and A. Priarone, "Improving the thermal performance of coaxial borehole heat exchangers," *Energy*, vol. 35, pp. 657–666, 2010.

[18] A. H. Tarrad, "A 3-Dimensional borehole numerical modeling for single and double U-tube ground-coupled heat pump," presented in COMSOL 2020 Conference, Grenoble, France, 2020.

[19] COMSOL Multiphysics version 5.4, *Heat Transfer Module User Guide*, 2018.

[20] D. Kim and S. Oh, "Optimizing the design of a vertical ground heat exchanger: Measurement of the thermal properties of bentonite-based grout and numerical analysis," *Sustainability*, vol. 10, no. 2664, pp. 1-15, 2018.

[21] Z. Sagia, A. Stegou, and C. Rakopoulos, "Borehole resistance and heat conduction around vertical ground heat exchangers," *The Open Chemical Engineering Journal*, vol. 6, pp. 32-40, 2012.

[22] Gaia Geothermal. *Ground Loop Design Software GLD*, (2009).

[23] S. Chen, J. Mao, X. Han, C. Li, and L. Liu, "Numerical analysis of the factors influencing a vertical U-tube ground heat exchanger," *Sustainability*, vol. 8, no. 882, pp. 1-12, 2016.

[24] Y. Wu, G. Gan, R. G. Gonzalez, A. Verhoef, and P. L. Vidale, "Prediction of the thermal performance of horizontal-coupled ground-source heat exchangers," *International Journal of Low-Carbon Technologies*, vol. 6, pp. 261–269, 2011.

[25] E. Zanchini, S. Lazzari, and A. Priarone, "Improving the thermal performance of coaxial borehole heat exchangers," *Energy*, vol. 35, pp. 657–666, 2010.

[26] R. B. Bird, W. E. Stewart, and E. N. Lightfoot, *Transport Phenomena*, 2nd ed. John Wiley, New York, 2002.

Ali H. Tarrad is a professor. He was awarded a BSc in mechanical engineering from Baghdad University/ Iraq in 1984. In 1991 he was awarded the Ph.D. degree in mechanical engineering from Heriot-Watt University/United Kingdom. He worked in the industrial field for 14 years as a thermal engineering specialist. The work included project management and planning in addition to the design tasks of the job. These projects covered many topics in the energy sector such as power plant technology, petroleum refinery industry, air conditioning and refrigeration systems, and the food industry. He worked in the education sector for 25 years as a tutor and research supervisor in the energy/power division-mechanical engineering in Iraq, Denmark, and France. His field of interest is related to energy management, sustainable energy (seawater and geothermal), waste energy recovery, heat pump technology, refrigeration, and heat transfer. He published many research articles in Scientific Journals and Conferences and supervised several MSc and Ph.D. theses.